Journal of Membrane Science 463 (2014) 166–172

Contents lists available at ScienceDirect

Journal of Membrane Science

journal homepage: www.elsevier.com/locate/memsci

# Oxygen-selective membranes integrated with oxy-fuel combustion

Wei Chen [a], Chu-sheng Chen [b], Henny J.M. Bouwmeester [a,b], Arian Nijmeijer [a], Louis Winnubst [a,b,*]

[a] Inorganic Membranes, Mesa+ Institute for Nanotechnology, University of Twente, P.O. Box 217, 7500 AE Enschede, The Netherlands
[b] CAS Key Laboratory of Advanced Materials for Energy Conversion and Department of Materials Science and Engineering, University of Science and Technology of China, Hefei, Anhui 230026, PR China

ARTICLE INFO

*Article history:*
Received 4 December 2013
Received in revised form
8 March 2014
Accepted 23 March 2014
Available online 29 March 2014

*Keywords:*
Oxy-fuel
Perovskite
Membrane
$CO_2$ tolerance

ABSTRACT

The perovskite-type oxide $SrCo_{0.8}Fe_{0.2}O_{3-\delta}$ (SCF), a highly oxygen-permeable material, is restricted for application in the membrane-integrated oxy-fuel combustion process by its low tolerance to $CO_2$. In the present work, we found that the $CO_2$ tolerance of SCF is improved by increasing the oxygen partial pressure in the $CO_2$-containing gas. Long term oxygen permeation experiments, at 950 °C, show that mixing 5% of oxygen into the $CO_2$ sweep gas effectively prevents degradation of the SCF membrane. X-ray photoelectron spectroscopy indicates that the increase in $CO_2$ tolerance of SCF is caused by a decrease in basicity of the material with increasing oxygen partial pressure. Based on these experimental results, a modified oxy-fuel combustion process is proposed. Calculation of the required membrane area for operating a 50 MW coal-fired power plant showed that the modified process comprises a viable option.



## 1. Introduction

Oxy-fuel combustion is a promising technique for $CO_2$ capture in a fossil fuel-fired power plant. In a typical oxy-fuel combustion process, pure oxygen instead of air is used for fuel combustion, resulting in a concentrated $CO_2$ gas stream, thus enabling efficient $CO_2$ capture. In most cases pure oxygen is separated from air via the cryogenic distillation or the pressure swing adsorption (PSA) process. Both processes are energy intensive, which limits further development of the oxy-fuel combustion technique [1,2]. It is proposed that oxygen can be produced by using mixed ionic-electronic conducting (MIEC) ceramic membranes, through which (neutral) oxygen transport at elevated temperatures (usually higher than 700 °C) [3,4]. A general scheme of this process is given in Fig. 1. The oxygen, as separated from air by the membrane, is carried by the sweep gas $CO_2$, while the $CO_2/O_2$ gas mixture is used to combust the fossil fuel. After combustion and purification, the exhaust gas mainly consists of $CO_2$ ( > 95%). Part of the $CO_2$ is recycled as sweep gas and the rest is compressed for delivery and storage.

Most MIEC materials have the perovskite crystal structure and contain alkaline-earth elements like Ca, Sr or Ba. Due to the presence of these elements, a carbonation reaction tends to occur when these membranes are exposed to a $CO_2$-containing atmosphere. This reaction results in the formation of an alkaline-earth carbonate layer on the membrane surface, which is impermeable for oxygen, resulting in a decline in oxygen flux or even to a non-permeating membrane. For example, $SrCo_{0.8}Fe_{0.2}O_{3-\delta}$ (SCF), a highly oxygen-permeable material, shows a decrease in oxygen flux to almost zero within 100 h when using $CO_2$ as sweep gas [5]. In order to increase the $CO_2$ tolerance of SCF membranes, $Sr^{2+}$ was partially substituted with $La^{3+}$ [6], or Co/Fe with $Ti^{4+}$, $Zr^{4+}$, $Ta^{5+}$ or $Nb^{5+}$ [7,8]. However, this improvement in $CO_2$ tolerance was at the expense of a decrease in oxygen flux [9].

Besides partial substitution, there are other parameters that affect the $CO_2$ tolerance of SCF, for example, temperature and $CO_2$ partial pressure ($pCO_2$). Yi et al. [10] found that SCF is more stable at higher temperature and lower $pCO_2$ (balanced with helium), and suggested SCF membranes should be operated above 900 °C. In the present study we examined another possible parameter: the oxygen partial pressure ($pO_2$), which has not been reported before to the best of our knowledge, as a way to improve the $CO_2$ tolerance of alkaline-earth containing perovskite materials. In this study thermal-gravimetric analysis (TGA) was used to investigate the effect of $pO_2$ on the stability of the SCF perovskite system in a $CO_2$-containing atmosphere. X-ray photoelectron spectroscopy (XPS) was used to examine the oxygen bonding energy of SCF at different oxygen partial pressures. Oxygen permeation experiments were performed to test the $CO_2$ tolerance of SCF membranes under operating conditions by adding 0% or 5% of oxygen to the sweep

* Corresponding author at: Inorganic Membranes, Mesa+ Institute for Nanotechnology, University of Twente, P.O. Box 217, 7500 AE Enschede, The Netherlands.
*E-mail address:* a.j.a.winnubst@utwente.nl (L. Winnubst).

http://dx.doi.org/10.1016/j.memsci.2014.03.063
0376-7388/

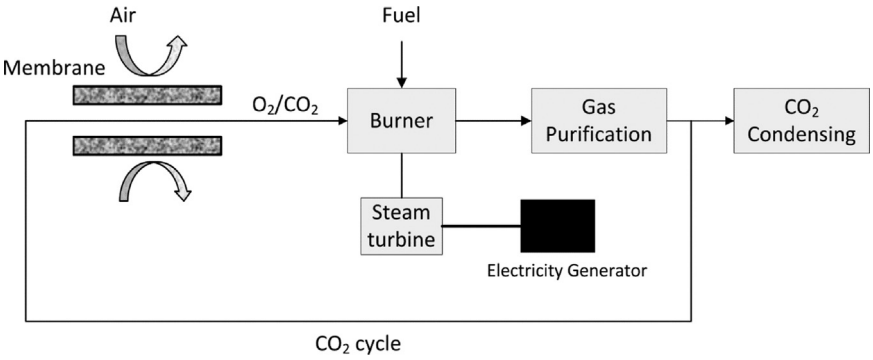


**Fig. 1.** Scheme for the membrane integrated oxy-fuel combustion process.

gas ($CO_2$). Finally, we propose a modified oxy-fuel combustion process and estimated the SCF membrane area needed in a combustion process for a 50 MW coal-fired power plant.

## 2. Experimental procedure and methodology

### 2.1. Sample preparation

$SrCo_{0.8}Fe_{0.2}O_{3-\delta}$ (SCF) was synthesized using an EDTA complexation/pyrolysis process. Metal nitrates were dissolved at a stoichiometric ratio in demineralized water under stirring. EDTA, dissolved in ammonium hydroxide, was added for chelating and after several minutes citric acid was added as well. The molar ratio of total metal ions:citric acid:EDTA was 1.0:1.5:1.0. The pH of the solution was adjusted to 6 by adding ammonium hydroxide. Subsequently $NH_4NO_3$ was added as an ignition aid at an amount of 100 g $NH_4NO_3$ per 0.1 mol of metal ions. The final solution was heated at 120–150 °C under stirring to evaporate water until the system changed into a viscous gel, which was transferred to a stainless steel vessel and heated on a hot plate at a temperature of around 500 °C, while a vigorous combustion took place, resulting in a fluffy powder. The powder was collected and calcined at 950 °C for 5 h at a heating and cooling rate of 3 °C/min. The calcined powders were uniaxially pressed at 4 MPa into disk-shaped membranes, subsequently cold isostatically pressed at 400 MPa for 6 min, and sintered in ambient air at 1200 °C for 10 h at a heating rate of 3 °C/min and a cooling rate of 2 °C/min.

### 2.2. Thermal-gravimetric analysis (TGA)

Isothermal gravimetric analyses were carried out on a Netzsch TG 449 F3 Jupiter®. About 45 mg of SCF powder was weighed in an alumina crucible and placed in the TGA setup. The system was heated (10 °C/min) to the desired temperature, in the range 900–1000 °C, in a flowing (120 ml/min) $O_2/N_2$ mixture at four different oxygen partial pressures ($pO_2$), namely $10^{-4}$, 0,05, 0.1 and 0.2 bar. The system was held at this temperature for 1 h to attain equilibrium. Next, the purge gas was switched to a mixture of $O_2/N_2$/67% $CO_2$ (flow rate 120 ml/min), keeping the oxygen partial pressure (and thus the oxygen flow rate) in the gas mixture identical as before switching (so respectively $10^{-4}$, 0,05, 0.1 and 0.2 bar), After 5 h, the system was cooled down at 20 °C/min in the same purge gas. All TGA data were processed with a correction file of a blank crucible using the same temperature program, to exclude background data of the equipment.

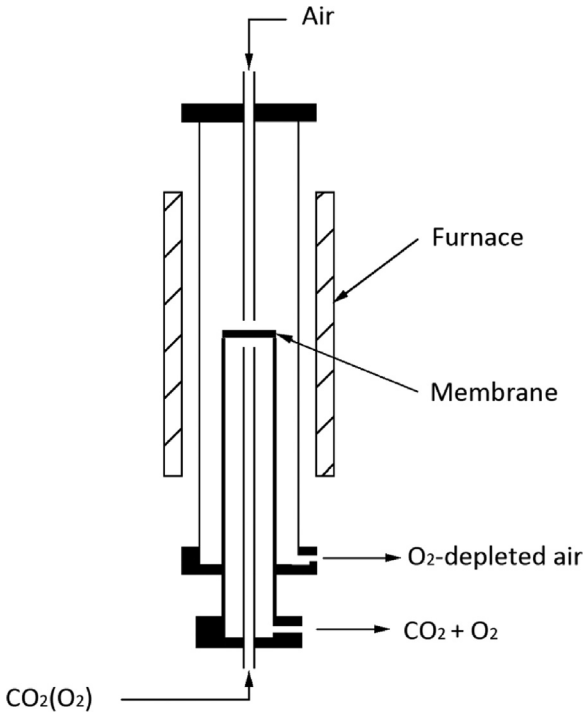


**Fig. 2.** Schematic diagram of the high temperature permeation setup.

### 2.3. X-ray photoelectron spectroscopy analysis

For X-ray photoelectron spectroscopy (XPS: ESCALAB MK II, VG equipment) analysis SCF bars (8 mm × 4 mm × 3 mm) were prepared using the same procedure as for the disk-shaped membranes. After sintering and polishing to the desired dimensions, the samples were annealed in nitrogen ($pO_2 = 10^{-4}$ bar) or oxygen ($pO_2 = 1.0$ bar) at 950 °C for 20 h and quenched to room temperature within a few seconds. Afterwards, the bars were fractured and only the center part of the cross section was analyzed by XPS using an X-ray beam size of 250 μm and a step size of 0.05 eV.

### 2.4. Oxygen permeation measurements

The experimental setup for oxygen permeation measurements is schematically shown in Fig. 2. Disk-shaped membranes with a diameter of 15 mm and a relative density > 90% were polished to a thickness of 1 mm and ultrasonically cleaned in ethanol. The membranes were sealed to one end of a quartz tube (diameter 12 mm) using gold paste and a sealing temperature of 1000 °C. After sealing, the temperature was lowered to 950 °C, and air was

applied as feed gas to one side of the membrane (100 ml/min), while $CO_2$ (50 ml/min) or a $CO_2/O_2$ gas mixture (50 ml/min) was applied to the other side to sweep away the permeated oxygen. The composition of the effluent gas at the permeate side was analyzed by an oxygen sensor (Systech ZR893). A gas chromatograph (Varian CP 4900 equipped with 5 Å molecular sieve column using He as carrier gas) was used to check for any leakage of the sealing. If there was no nitrogen peak in the spectrum for the permeate gas stream, it was assumed that the sealing was sufficient and oxygen permeation due to leakage was neglected.

### 2.5. Membrane area calculation

The aim of this calculation is to estimate the membrane area needed for a 50 MW coal-fired power plant. This was done in two steps: (1) calculation of the oxygen produced by a single membrane tube and (2) determination of the total required membrane area, necessary for the power plant, based on the calculation for a single tube.

#### 2.5.1. Oxygen production by a single membrane tube

Tubular membranes were chosen in this study and a simple scheme of the membrane module and a membrane tube is shown in Fig. 3. For the calculation the oxygen production by a single membrane tube, the following assumptions are made: (1) oxygen is transported from the shell side to the core side of the membrane tube; (2) the sweep and feed gas flows are in a counter-current mode; (3) there is no oxygen concentration polarization in the radial direction; (4) the absolute pressure drop in the membrane module is neglected; (5) the oxygen transport in both core and shell side of the membrane is described by a convection diffusion and a reaction model (Eqs. (1) and (2)) [11]; and (6) the oxygen flux is governed by Wagner's equation (Eq. (3)) [12], in which the electronic conductivity of the membranes is predominant and the ionic conductivity constant.

$$D_s\frac{d^2 f_s}{d z^2}-\frac{d}{d z}(\vec{v}_s f_s)+\frac{2V_m}{R_1}\vec{J}_{O_2}=0 \tag{1}$$

$$D_f\frac{d^2 f_f}{d z^2}-\frac{d}{d z}(\vec{v}_f f_f)+\frac{2R_1 V_m}{R_2{}^2-R_1{}^2}\vec{J}_{O_2}=0 \tag{2}$$

where

$$\begin{cases}\vec{J}_{O_2}=\frac{RT}{(4F_a)^2 d}\sigma_{ion}\ln\left(\frac{P_f f_f}{P_s f_s}\right)\\ \vec{v}_s=\frac{\vec{F}_s}{\pi R_1^2}\\ \vec{v}_f=\frac{\vec{F}_f}{\pi(R_2^2-R_1^2)}\end{cases} \tag{3}$$

with Danckwerts boundary conditions [13],

$$\begin{cases}\vec{v}_s f_s^i=\vec{v}_s f_s-D_s\frac{d f_s}{d z}, & z=0\\ \frac{d f_s}{d z}=0, & z=L\\ \frac{d f_f}{d z}=0, & z=0\\ \vec{v}_f f_f^i=\vec{v}_f f_f-D_f\frac{d f_f}{d z}, & z=L\end{cases} \tag{4}$$

where $f$, $D$, $P$, $F$ and $\vec{v}$ are $O_2$ mole fractions, $O_2$ is diffusion coefficient in the gas phase, absolute pressure, volume flow rate and velocity of the sweep (with subscript s) gas or feed (with subscript f) gas; $R$ is gas constant, $z$ is the coordinates along the membrane tube, $T$ is absolute temperature, $V_m$ is molar volume of oxygen in the gas phase oxygen at given temperature and pressure, $F_a$ is Faraday constant, $d$ is membrane thickness, $\sigma_{ion}$ is oxygen ionic conductivity, $R_1$ is the radius of the tube membrane (average of outer and inner diameter) and $R_2$ is the distance from center of the tube membrane to the wall boundary (Fig. 3). $f_s^i$, $f_f^i$, $f_s^i$ and $f_f^i$ are the $O_2$ mole fractions at the inlet (with superscript i) and outlet (with superscript o) of sweep gas and feed gas and $L$ the length of the membrane tube.

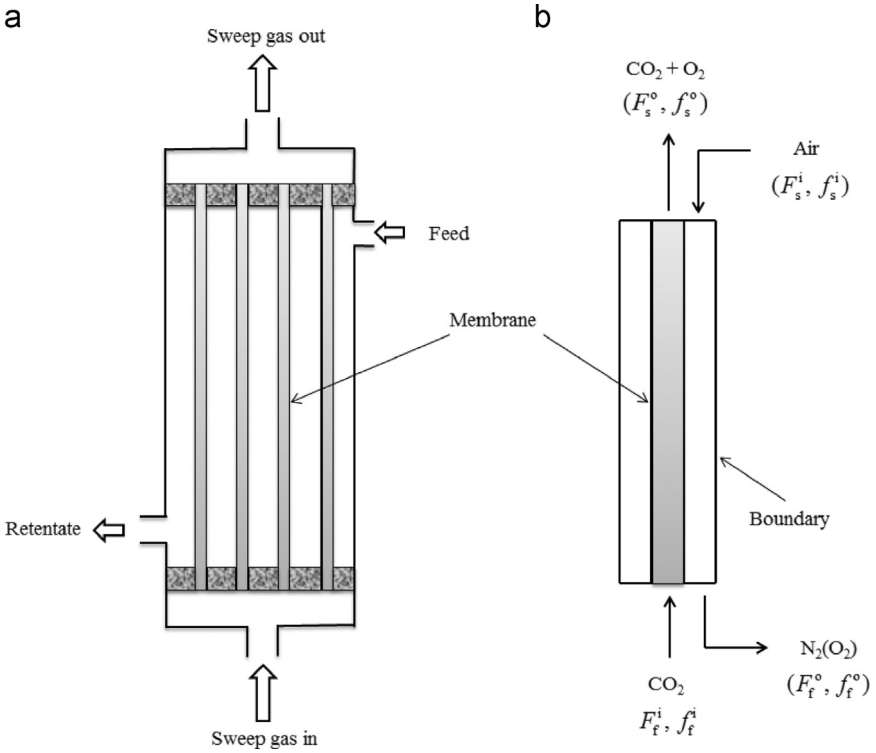


**Fig. 3.** Schematic drawing of: (a) a membrane module and (b) a membrane tube.

Eq. (1) and (2), in combination with the boundary conditions as given in eq. (4), can be numerically solved if sweep/feed gas flow rates ($F$) and their $O_2$ mole fractions ($f$) at the inlet of the membrane tube are known ($F_s^i, F_f^i, f_s^i, f_f^i$). From these results gas flow rates and $O_2$ mole fractions at the outlet of the membrane tube can be calculated ($F_s^o, F_f^o, f_s^o, f_f^o$). In most cases, $f_s^i$ and $f_f^i$ are fixed, while $F_s^i$ and $F_f^i$ can be adjusted if necessary. For example, if a certain $O_2$ mole fractions ($f_s^o, f_f^o$) in the sweep/feed gas at the outlet of the membrane tube is required, appropriate $F_s^i$ and $F_f^i$ values have to be chosen. In this study. In this work $f_s^o$ is fixed at a value of 0.35 because it has been reported that a composition of approximately 35% $O_2$ and 65% of $CO_2$ (v/v) is needed in an oxy-fuel combustion process to ensure the flame temperature and heat capacity of gases to match fuel combustion in air [14]. Besides, $f_f^o$ is kept at a value of 0.02 which means that around 92% of oxygen in the air is recovered.

As the increase of sweep gas flow rate is caused by the permeated oxygen, the amount of moles of oxygen produced by a single membrane tube, $F_{O_2}$, can be calculated with the following equation:

$$F_{O_2} = F_s^o - F_s^i \tag{5}$$

#### 2.5.2. Total membrane area calculation

The total membrane area is based on a 50 MW coal-fired power plant. In this power plant, the combustion of coal is described by reaction (6) assuming coal contains 100% of carbon.

$$C + O_2 \rightarrow CO_2 \tag{6}$$

If it is further assumed that the heat density of coal is 30 MJ/kg (HHV) and the overall efficiency of the power plant is 30% [15], the total amount of coal needed for one hour operation of this power plant is

$$N_{coal} = \frac{50\ \text{MW} \times 3600\ \text{s}}{30\ \text{MJ/kg} \times 0.3 \times 12\ \text{kg/kmole}} \approx 1667\ \text{kmole} \tag{7}$$

The oxygen needed for the combustion of coal has the same mole number. Since the oxygen produced by a single tube membrane is known (Eq. (5)), the number of tubular membranes, $N_m$, and also the total membrane area, $A$, can be calculated

$$N_m = \frac{F_{O_2}^T}{F_{O_2}} \tag{8}$$

$$A = 2\pi R_1 L N_m \tag{9}$$

where $F_{O_2}^T$ is the amount of total oxygen needed and $F_{O_2}$ is the amount of oxygen produced by a single membrane tube.

## 3. Results and discussion

### 3.1. Thermal-gravimetric analysis

The calcined SCF powder was checked to have a phase pure perovskite crystal structure by means of XRD. The reaction between SCF and $CO_2$ was studied by isothermal gravimetric experiments TGA. In Fig. 4a, the results of TGA experiments at 950 °C are described under varying $pO_2$ by adjusting the $N_2/O_2$ ratio and keeping the $pCO_2$ constant at 0.67 bar. The weight of the SCF powder samples immediately increases upon exposure to a $CO_2$-containing gas mixture, while the rate of weight gain is different when the experiments were performed at different $pO_2$ ($10^{-4}$, 0.05, 0.10 and 0.20 bar); a higher $pO_2$ leads to a lower reaction rate of $CO_2$ with the SCF powder sample. After 5 h, the weight of the samples increased by 16.9%, 9.0%, 6.9% and 4.5% respectively. Clearly, the reaction between SCF and $CO_2$ at 950 °C is strongly affected by $pO_2$.

Another parameter that can influence the reaction between SCF and $CO_2$ is the temperature. At 1000 °C, the reaction was very slow, and after 5 h, the weight only increased by 0.6%, compared to 8.5% and 6.9% for 900 °C and 950 °C, respectively, when using a $pO_2$ of 0.1 bar. A higher temperature leads to a lower reaction rate (Fig. 4b), which indicates that SCF is more stable at higher temperatures. This result is in accordance with previous data of Yi et al. [10]. A similar trend has been found for other perovskite structures like $BaCe_{0.9}Y_{0.1}O_{3-\delta}$ [16]. A thermodynamic analysis has been performed by Brandão et al. [17] for the explanation of this temperature effect.

### 3.2. XPS analysis

The inhibition of the reaction between SCF and $CO_2$ can be explained by the Lewis acid–base theory, where $CO_2$ is regarded as the gas acid and SCF as the solid base [5]. The intensity of this reaction is determined by the basicity of SCF, which may be different under different conditions, for example, different temperature or $pO_2$. In general, the basicity of a metal oxide is defined as its ability to donate electrons to an adsorbed molecule (in this case $CO_2$). The O1s binding energy (O1s BE), which is related to the charge density around the

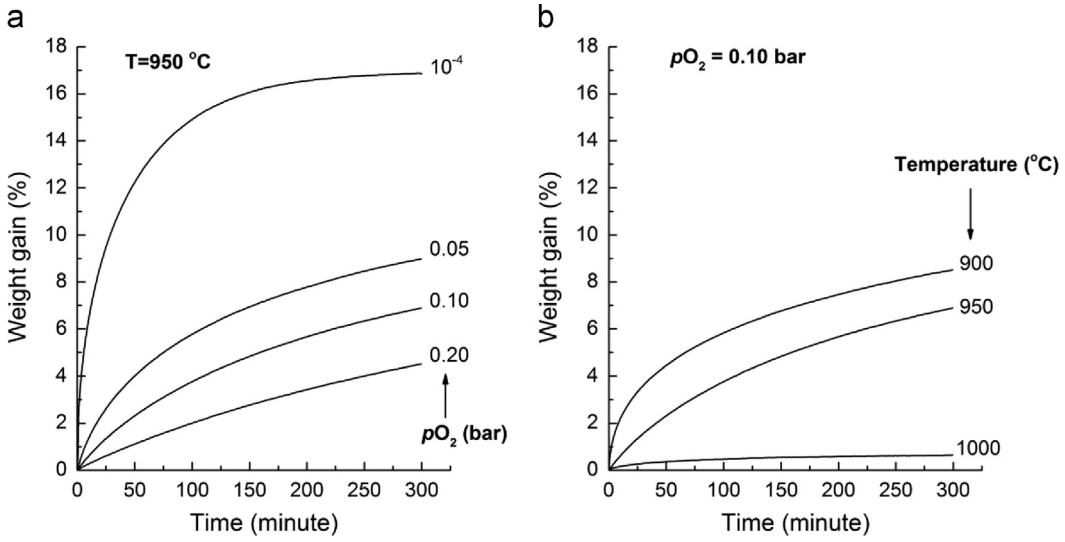


**Fig. 4.** Weight gain of SCF powder samples as a function of time at different values of: (a) $pO_2$ and (b) temperature ($pCO_2$ = 0.67 bar in all cases and balance: $N_2$).

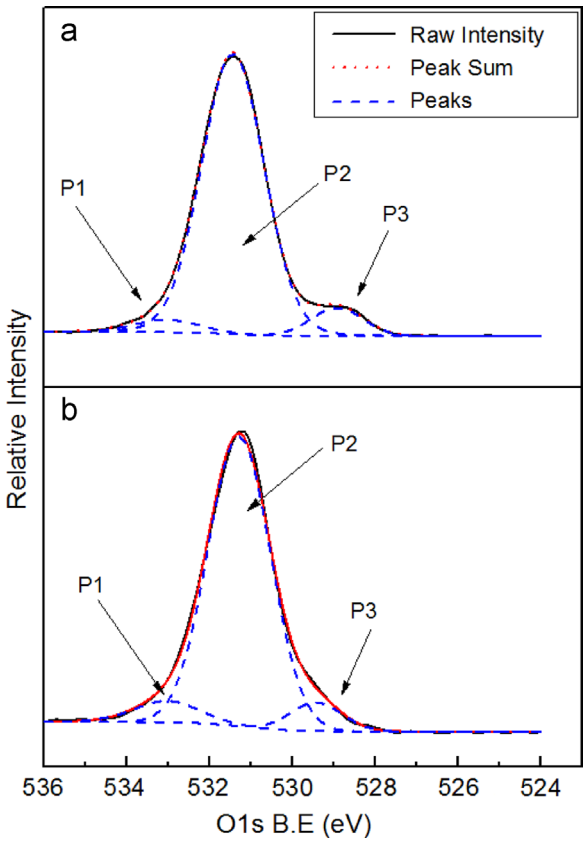


**Fig. 5.** XPS spectrum of the SCF samples quenched from 20 h's annealing at 950 °C and in a $pO_2$ of: (a) $10^{-4}$ bar and (b) 1.0 bar. Cross section of the fractured samples was used for the measurement. P1, P2 and P3 represent the O1s binding energies of: absorbed water, absorbed oxygen and lattice oxygen.

**Table 1**
Peak positions of the XPS spectrum as given in Fig. 5.

| $pO_2$ (bar) | P1 (eV) | P2 (eV) | P3 (eV) |
|---|---|---|---|
| $1 \times 10^{-4}$ (Fig. 5a) | 533.0 | 531.4 | 528.9 |
| 1.0 (Fig. 5b) | 533.0 | 531.4 | 529.5 |

oxide ions, is usually taken as a measure of the basicity of a metal oxide [18,19]. A higher O1s BE means a lower charge density and, consequently, it is more difficult for the oxides to donate electrons to the adsorbed molecules [20], indicating a lower basicity of the metal oxide. To check whether the O1s BE for SCF is $pO_2$ dependent, we annealed SCF bulk samples in oxygen ($pO_2 = 1$ bar) and nitrogen ($pO_2 = 10^{-4}$ bar) at 950 °C for 20 h and quenched them to room temperature. XPS analysis was used to determine the O1s BE. The raw XPS data were de-convoluted into three Gaussian peaks (Fig. 5). The peak at 533.0 eV is assigned to oxygen in absorbed water, 531.4 eV to absorbed oxygen, and 528–530 eV to lattice oxygen [21,22]. As we can see from Table 1, for absorbed water and oxygen, the O1s BE has the same value in both $pO_2$ cases, and are consistent with data reported in previous studies [5,7], for the lattice oxygen an increase in O1s BE from 528.9 eV to 529.5 eV was observed when $pO_2$ was increased from $10^{-4}$ to 1 bar. This suggests that the basicity of SCF tends to be lower at higher $pO_2$, thus lowers the affinity of reaction between SCF and $CO_2$. Similar correlation between $CO_2$ tolerance and O1s binding energy has been reported by Zeng et al. [5] on the Ti-doped SCF system.

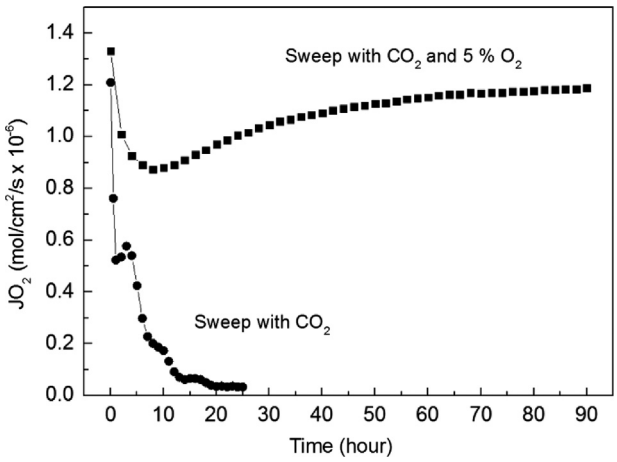


**Fig. 6.** Long-term oxygen permeation tests of SCF membranes at 950 °C by using pure $CO_2$ (circles) or an $O_2/CO_2$ mixture (squares, $O_2$ mole fraction 5%) as sweep gas (50 ml/min for both cases). Feed gas: air. Membrane thickness: 1 mm.

### 3.3. Oxygen permeation measurements

To check the stability of SCF membranes in $CO_2$ under operating conditions, two long term (90 h) oxygen permeation measurements were performed, at 950 °C, in $CO_2$ atmosphere. In the first experiment synthetic air ($O_2$ 20 ml/min and $N_2$ 80 ml/min) was used as feed gas, and pure $CO_2$ (50 ml/min, $pO_2 \approx 10^{-4}$ bar) was used as sweep gas. In the second experiment, a mixture of $O_2/CO_2$ ($O_2$ 5 ml/min and $CO_2$ 45 ml/min) was used as sweep gas, and the feed gas was partly changed ($O_2$ 50 ml/min and $N_2$ 50 ml/min) to ensure a comparable $pO_2$ gradient across the membrane for both experiments. The results of oxygen permeation measurements, as given in Fig. 6, show that the SCF membranes behaved quite differently in pure $CO_2$ than in the $CO_2/O_2$ mixture. If pure $CO_2$ is used as sweep gas, the oxygen flux decreased quickly to zero within 25 h. A similar result has also been reported by Zeng et al. [5]. By using an $O_2/CO_2$ mixture ($pO_2 = 0.05$ bar) as sweep gas, the oxygen flux decreased by 34% in the first 10 h, and slowly recovered to 90% of its original value in the following 50 h, and then became constant. Although it is still not clear what caused the oxygen flux decrease in the first 10 h, it is obvious that the addition of some oxygen to the sweep gas indeed enhances the $CO_2$ tolerance of SCF membranes in a $CO_2$ atmosphere under operating conditions, and thus prevented the oxygen flux from decreasing in the long run. However, as shown in Fig. 4, the reaction between SCF powder and $CO_2$ could not be prevented at a temperature of 950 °C by increasing $pO_2$ up to 0.20 bar, which seems to be in conflict with the oxygen permeation results. This "conflict" is attributed to the dynamic process occurring at the permeate side of the membrane. During an oxygen permeation experiment, oxygen is released from the membrane surface at the permeate side in the form of oxygen molecules, creating a higher oxygen activity at the membrane interface than in the gas bulk phase [23,24]. This dynamic process, which is different from the stationary environment in the TGA experiments, is beneficial for the membrane stability.

### 3.4. Process design and membrane area calculation

Based on these experimental results we propose a new design for a membrane integrated oxy-fuel combustion process (Fig. 7). In this concept an extra $CO_2/O_2$ recycle is introduced to increase the $pO_2$ in the $CO_2$ sweep gas. This modification ensures that the $pO_2$ in the $CO_2$ sweep gas at the inlet of the membrane module is high enough to protect SCF from degradation by carbonation. However, this modification also leads to an increase of needed membrane area because part of $CO_2/O_2$ gas stream is used for

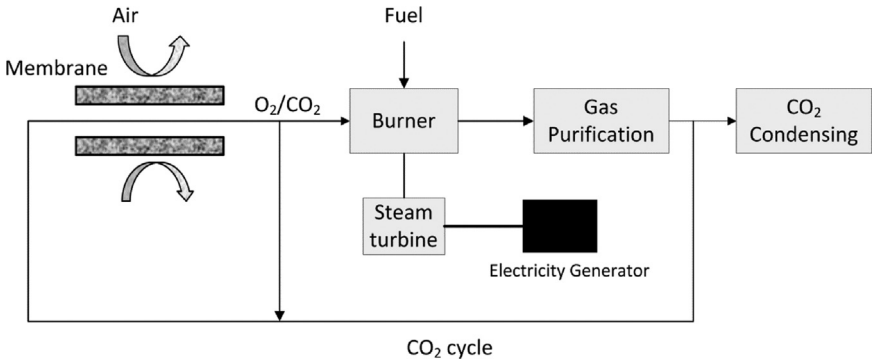


**Fig. 7.** A modified process scheme for the membrane integrated oxy-fuel combustion.

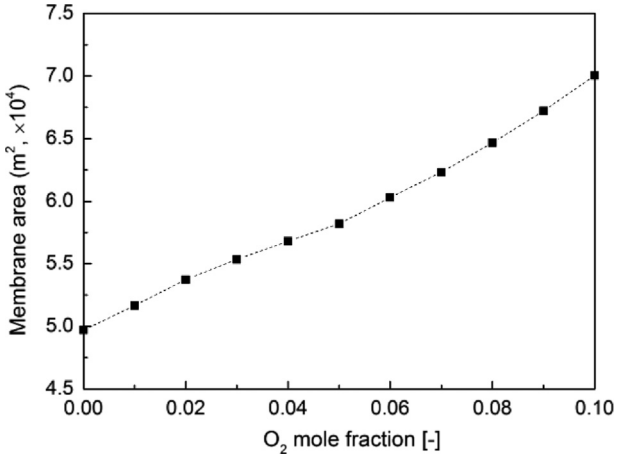


**Fig. 8.** Calculated SCF membrane area for a 50 MW coal-fired power plant with different $O_2$ mole fractions $CO_2$ in the sweep gas.

**Table 2**
Membrane geometry and operating conditions of oxygen permeation in a single membrane tube.

| Variable | Value | Units |
|---|---|---|
| Membrane length ($L$) | 100 | cm |
| Membrane outer diameter | 1.0 | cm |
| Membrane inner diameter | 0.8 | cm |
| Ionic conductivity | 1.0 | S/cm |
| Feed side pressure | 10 | bar |
| Sweep side pressure | 1.7[a] | bar |
| Temperature | 1223 | K |
| Diffusion coefficient of $O_2/N_2$ | 2.19[b] | $cm^2/s$ |
| Diffusion coefficient of $O_2/CO_2$ | 1.55[b] | $cm^2/s$ |
| $O_2$ mole fraction of feed gas at inlet ($f_f^i$) | 0.209 | – |
| $O_2$ mole fraction of sweep gas at inlet ($f_s^i$) | 0.005–0.1 | – |
| $O_2$ mole fraction of feed gas at outlet ($f_f^o$) | 0.02 | – |
| $O_2$ mole fraction of sweep gas at outlet ($f_s^o$) | 0.35 | – |

[a] Typical pressure for oxy-fuel application [1].
[b] The binary diffusion coefficients of $O_2/N_2$ and $O_2/CO_2$ at 950 °C were calculated with Chapman–Enskog's theory [25].

recycling and the driving force for oxygen permeation is also slightly decreased. In order to quantitatively study this effect, a calculation was performed of the total membrane area needed for a 50 MW coal-fired power plant using $O_2$ mole fractions in the $CO_2$ sweep varying from 0.005 to 0.1 (details about this calculation can be found in the experimental procedure and methodology section). The membrane geometry and operating conditions are listed in Table 2, and the results of calculation are given in Fig. 8. When $f_s^i$ ($O_2$ mole fraction in $CO_2$ sweep gas) is increased to 0.05, which has been proven to be sufficient to protect SCF membranes against $CO_2$ degradation, the total needed membrane area increases from $4.97 \times 10^4$ to $5.81 \times 10^4$ $m^2$, so only by ~17% compared with the (theoretical) case of using pure $CO_2$ as sweep gas

## 4. Conclusion

This study demonstrates that degradation of $SrCo_{0.8}Fe_{0.2}O_{3-\delta}$ (SCF) perovskite, oxygen-selective, membranes in a $CO_2$ atmosphere is affected by the oxygen partial pressure in the $CO_2$ sweep gas. Increasing the oxygen partial pressure enhances the $CO_2$ tolerance of these membranes. Long term oxygen permeation tests at 950 °C showed that mixing 5% of oxygen to the $CO_2$ sweep gas can prevent the SCF membrane from degradation without sacrificing its high oxygen permeability. Based on these experimental results a modified membrane integrated oxy-fuel combustion process is proposed. A simple membrane area calculation shows that 17% of additional membrane area is necessary for achieving the same oxygen yield compared with pure $CO_2$ as sweep gas.

## Acknowledgments

Wei Chen thanks the China Scholarship Council for the financial support of his Ph.D. Project.

## References

[1] B. Metz, O. Davidson, H.d. Coninck, M. Loos, L. Meyer, IPCC Special Report on Carbon Dioxide Capture and Storage, Intergovernmental Panel on Climate Change, 2005.
[2] M.A. Habib, H.M. Badr, S.F. Ahmed, R. Ben-Mansour, K. Mezghani, S. Imashuku, G.J. la O, Y. Shao-Horn, N.D. Mancini, A. Mitsos, P. Kirchen, A.F. Ghoneim, A review of recent developments in carbon capture utilizing oxy-fuel combustion in conventional and ion transport membrane systems, Int. J. Energy Res. 35 (2011) 741–764.
[3] S. Engels, F. Beggel, M. Modigell, H. Stadler, Simulation of a membrane unit for oxyfuel power plants under consideration of realistic BSCF membrane properties, J. Membr. Sci. 359 (2010) 93–101.
[4] Y. Teraoka, H.-M. Zhang, S. Furukawa, N. Yamazoe, Oxygen permeation through perovskite-type oxides, Chem. Lett. 14 (1985) 1743–1746.
[5] Q. Zeng, Y.B. Zu, C.G. Fan, C.S. Chen, $CO_2$-tolerant oxygen separation membranes targeting $CO_2$ capture application, J. Membr. Sci. 335 (2009) 140–144.
[6] T. Klande, O. Ravkina, A. Feldhoff, Effect of A-site lanthanum doping on the $CO_2$ tolerance of $SrCo_{0.8}Fe_{0.2}O_{3-\delta}$ oxygen-transporting membranes, J. Membr. Sci. 437 (2013) 122–130.
[7] W. Chen, C.S. Chen, L. Winnubst, Ta-doped $SrCo_{0.8}Fe_{0.2}O_{3-\delta}$ membranes: phase stability and oxygen permeation in $CO_2$ atmosphere, Solid State Ionics 196 (2011) 30–33.

[8] G. Zhang, Z. Liu, N. Zhu, W. Jiang, X. Dong, W. Jin, A novel $Nb_2O_5$-doped $SrCo_{0.8}Fe_{0.2}O_{3-\delta}$ oxide with high permeability and stability for oxygen separation, J. Membr. Sci. 405–406 (2012) 300–309.
[9] J.W. Stevenson, T.R. Armstrong, R.D. Carneim, L.R. Pederson, W.J. Weber, Electrochemical properties of mixed conducting perovskites $La_{1-x}M_xCo_{1-y}Fe_yO_{3-\delta}$ ($M$=Sr, Ba, Ca), J. Electrochem. Soc. 143 (1996) 2722–2729.
[10] J.X. Yi, S.J. Feng, Y.B. Zuo, W. Liu, C.S. Chen, Oxygen permeability and stability of $Sr_{0.95}Co_{0.8}Fe_{0.2}O_{3-\delta}$ in a $CO_2$- and $H_2O$-containing atmosphere, Chem. Mater. 17 (2005) 5856–5861.
[11] B. Bird, W. E Stewart, E. N Lightfoot, Transport Phenomena, 2nd ed., John Wiley & Sons, Inc., 2001.
[12] Y.S. Lin, W.J. Wang, J.H. Han, Oxygen permeation through thin mixed-conducting solid oxide membranes, AIChE J. 40 (1994) 786–798.
[13] P.V. Danckwerts, Continuous flow systems: distribution of residence times, Chem. Eng. Sci. 2 (1953) 1–13.
[14] E. Croiset, K. Thambimuthu, A. Palmer, Coal combustion in $O_2/CO_2$ mixtures compared with air, Can. J. Chem. Eng. 78 (2000) 402–407.
[15] J. Black, Cost and performance baseline for fossil energy plants, Volume 1: Bituminous Coal and Natural Gas to Electricity Final Report, National Energy Technology Laboratory (2007) 626.
[16] N. Zakowsky, S. Williamson, J.T.S. Irvine, Elaboration of $CO_2$ tolerance limits of $BaCe_{0.9}Y_{0.1}O_{3-\delta}$ electrolytes for fuel cells and other applications, Solid State Ionics 176 (2005) 3019–3026.
[17] A. Brandão, J.F. Monteiro, A.V. Kovalevsky, D.P. Fagg, V.V. Kharton, J.R. Frade, Guidelines for improving resistance to $CO_2$ of materials for solid state electrochemical systems, Solid State Ionics 192 (2011) 16–20.
[18] H. Vinek, H. Noller, M. Ebel, K. Schwarz, X-ray photoelectron spectroscopy and heterogeneous catalysis, with elimination reactions as an example, J. Chem. Soc. Faraday Trans. 1 Phys. Chem. Condens. Ph. 73 (1977) 734–746.
[19] H. Noller, J.A. Lercher, H. Vinek, Acidic and basic sites of maim group mixed metal oxides, Materi. Chem. Phys. 18 (1988) 577–593.
[20] H.J.M. Bosman, A.P. Pijpers, A.W.M.A. Jaspers, An X-ray photoelectron spectroscopy study of the acidity of $SiO_2$–$ZrO_2$ mixed oxides, J. Catal. 161 (1996) 551–559.
[21] C.M. Pradier, C. Hinnen, K. Jansson, L. Dahl, M. Nygren, A. Flodstrom, Structural and surface characterization of perovskite-type oxides; influence of A and B substitutions upon oxygen binding energy, J. Mater. Sci. 33 (1998) 3187–3191.
[22] N.A. Merino, B.P. Barbero, P. Eloy, L.E. Cadús, $La_{1-x}Ca_xCoO_3$ perovskite-type oxides: identification of the surface oxygen species by XPS, Appl. Surf. Sci. 253 (2006) 1489–1493.
[23] J. Sunarso, S. Baumann, J.M. Serra, W.A. Meulenberg, S. Liu, Y.S. Lin, J.C.D. da Costa, Mixed ionic-electronic conducting (MIEC) ceramic-based membranes for oxygen separation, J. Membr. Sci. 320 (2008) 13–41.
[24] H.J.M. Bouwmeester, H. Kruidhof, A.J. Burggraaf, Importance of the surface exchange kinetics as rate limiting step in oxygen permeation through mixed-conducting oxides, Solid State Ionics 72 (1994) 185–194.
[25] E.L Cussler, Diffusion: Mass Transfer in Fluid System, 1st ed., Cambridge University Press, Cambridge, 1984.